NATIONAL ADVISORY COMMITTEE
FOR AERONAUTICS

TECHNICAL NOTE 3230

INVESTIGATION OF DISTRIBUTED SURFACE ROUGHNESS

ON A BODY OF REVOLUTION AT A

MACH NUMBER OF 1.61

By K. R. Czarnecki, Ross B. Robinson,
and John H. Hilton, Jr.

Langley Aeronautical Laboratory
Langley Field, Va.

Washington

June 1954

NATIONAL ADVISORY COMMITTEE FOR AERONAUTICS

TECHNICAL NOTE 3230

INVESTIGATION OF DISTRIBUTED SURFACE ROUGHNESS

ON A BODY OF REVOLUTION AT A

MACH NUMBER OF 1.61

By K. R. Czarnecki, Ross B. Robinson,
and John H. Hilton, Jr.

SUMMARY

An investigation has been made of the effects of distributed sur-
face roughness, consisting of lathe-tool marks, on the skin-friction
drag of a body of revolution at a Mach number of 1.61. The tests were
made on ogive-cylinders at zero angle of attack over a roughness range
from 23 to 480 microinches root mean square and over a Reynolds number
range from 2.5×10^6 to 37×10^6.

The results indicate that the effects of surface roughness at a
Mach number of 1.61 are generally similar to those found at subsonic
speeds. Both the allowable roughness height for a turbulent boundary
layer and the variation with Reynolds number of the increment in skin-
friction drag due to roughness are in good agreement with Nikuradse's
low-speed data. At constant velocity, the allowable roughness height
is nearly independent of model length and dependent primarily upon
changes in Reynolds number per foot. As an approximation, in inches
root mean square,

Allowable roughness height = $19.8 \times$ (Reynolds number per foot)$^{-0.9}$

An increase in surface roughness caused a small decrease in the
Reynolds number for transition at the model base for the ogive-cylinders
tested and had little or no effect on surface-temperature-recovery fac-
tors for the laminar or turbulent boundary layers. Pressure gradients
or body shapes apparently have little or no effect on the average skin-
friction drag coefficient for smooth bodies of high fineness ratio when
the boundary layer is turbulent.

INTRODUCTION

The basic laws of skin friction on rough surfaces were established by Nikuradse about 1933 by means of tests of rough pipes with water. These results are translated in reference 1. Shortly thereafter, Prandtl and Schlichting (ref. 2) showed how the pipe results could be applied to a flat plate. This information, however, found little practical use in aeronautics at that time because the airplanes of that date had very high form drag and relatively low maximum speeds and these factors precluded any sizable effects due to surface roughness. As airplanes became more streamlined and their maximum speeds increased, surface-roughness effects became important and numerous investigations of these effects were made at subsonic speeds. With the attainment of supersonic speeds, surface-roughness effects take on increased importance, not only from the standpoint of skin-friction drag but also because of the increased rates of heat transfer that may be expected. However, prior to the present work no research on roughness effects at supersonic speeds had been conducted. The purpose of this investigation was to determine the effects of distributed roughness on the drag of a body of revolution at a Mach number of 1.61 for comparison and correlation with the available subsonic information.

The investigation was conducted in the Langley 4- by 4-foot supersonic pressure tunnel on four ogive-cylinder models having nominal distributed surface roughness, generated by lathe tools, of 23, 85, 240, and 480 microinches root mean square. The models were identical in shape and had an ogival nose 3 calibers in length and an overall fineness ratio of 12.2. Tests were made at zero angle of attack with natural transition and with transition fixed near the model nose over a Reynolds number range from about 2.5×10^6 to about 37×10^6, based on body length. On the models with roughnesses of 23 and 480 microinches, the surface-temperature—recovery-factor distribution was also determined for the same range of test conditions. The resulting skin-friction data are compared with Nikuradse's low-speed results.

SYMBOLS

C_{D_T} total drag coefficient, D/qS_f

C_{D_B} base drag coefficient, $\dfrac{p_B - p_1}{q_1}$

C_{D_P} forebody pressure-drag coefficient, $\dfrac{\text{Forebody pressure drag}}{qS_f}$

C_{f_f} skin-friction drag coefficient based on S_f, $C_{D_T} - C_{D_B} - C_{D_P}$

C_{f_W} skin-friction drag coefficient based on S_W, $C_{f_f} \dfrac{S_f}{S_W}$

ΔC_{f_W} incremental skin-friction coefficient with turbulent boundary layer, $\left(C_{f_W}\right)_{\text{rough model}} - \left(C_{f_W}\right)_{\text{smooth model}}$

D total drag

L model length

d model diameter

S_f maximum frontal area of model

S_W total wetted area of model

x longitudinal distance along model axis from nose

k roughness height, root-mean-square values

k' roughness height, absolute values, $\dfrac{1}{0.707} k$

M Mach number

U velocity of free stream

ν kinematic viscosity

R Reynolds number, UL/ν

R_{ft} Reynolds number per foot

q dynamic pressure

p static pressure

δ_L thickness of laminar sublayer

T temperature, °F abs

T_S equilibrium surface temperature, zero heat transfer, °F abs

r temperature-recovery factor, defined by $T_S = T_l\left(1 + r\,\dfrac{\gamma - 1}{2}\,M_l^2\right)$

γ ratio of specific heats of air, 1.40

Subscripts:

ad   admissible or allowable

B   base

l local conditions just outside boundary layer

L   laminar sublayer

tr   transition

1   free stream

APPARATUS AND METHODS

Wind Tunnel

The tests were made in the Langley 4- by 4-foot supersonic pressure tunnel. Calibration of the test-section flow at $M = 1.61$ indicates a Mach number variation of about ±0.01 and no significant flow irregularities in the stream flow direction. The turbulence level in the test section is not known, but for all stagnation pressures it is less than 0.9 percent of the flow velocity in the subsonic flow some distance upstream of the first minimum (ref. 3).

Models

The aluminum models were bodies of revolution composed of a 3-caliber ogive nose and a cylindrical afterbody (see fig. 1). Approximately constant, uniformly distributed roughness was produced by lathe-tool marks on the entire surface of each model (fig. 2), except near the nose (approximately the first 2 in.) where control of the roughness was impossible. The average roughness, dimensions, and areas of the models are given in table 1. Surface roughness of the models was measured in microinches, root mean square, by means of a Physicists Research Co. Profilometer, Model No. 11.

The models were sting mounted. Total-drag measurements were made with a single-component strain-gage balance. Actually, because of the failure of two sets of drag beams, three separate balances were used in the course of the tests. Base pressures were measured with a single tube well inside the model and by taking an average of the values given by three tubes spaced radially in the plane of the base. Skin temperatures were measured with two longitudinal rows of thermocouples connected to Brown self-balancing potentiometers. The rows were 180° apart, one containing 15 thermocouples and the other containing 5. The longitudinal position of the thermocouples is given in table 2. The first 12 thermocouples were on one potentiometer, the last 8 on another.

A cylindrical wooden block approximately the same diameter as the models and 4 inches long was positioned about 1/8 inch back of the model base for tests of the models with roughness of 23 and 480 microinches to reduce the load on the balance at high stagnation pressures. A higher capacity balance installed in the models with roughness of 85 and 240 microinches made the blocks unnecessary for tests of these configurations.

Tests

All tests were made with the models at zero angle of attack through a stagnation-pressure range from 2 to about 33 lb/sq in. abs, corresponding to Reynolds numbers based on model length of about 2.5×10^6 to 37×10^6. Tunnel stagnation temperatures varied from about 95° F to 125° F, depending on the stagnation pressure. The tunnel dewpoint was sufficiently low to prevent significant condensation effects.

Drag and base-pressure data were taken through the Reynolds number range on all the models with natural and fixed transition. Transition was fixed about 1/2 inch back of the nose of the model with No. 60 carborundum grains cemented to the model surface. Temperature measurements for the condition of zero heat transfer were made through the Reynolds number range on the models with roughness of 23 and 480 microinches with natural and fixed transition.

One group of runs was made with sandpaper on various parts of the cylindrical afterbody of the 23-microinch-roughness model with transition fixed near the nose. Number 6/0 garnet paper, having a roughness of about 400 microinches root mean square was glued to the model and faired smoothly into the surface. Tests were made with the front half, the rear half, and all the cylinder covered.

Considerable difficulty was encountered in obtaining accurate body-drag measurements with natural transition at high Reynolds numbers because of the "sandblast" action of particles in the tunnel airstream.

The pits and peaks produced by these particles on the soft surface were removed as completely as possible and several repeat runs made with each model in an attempt to obtain data free of sandblast effects.

The tests were made in two parts, series A and series B, because of failure of the tunnel drive equipment. The first set of force and pressure measurements made on the 23- and 480-microinch-roughness models and all the temperatures obtained on the 23-microinch-roughness model are designated series A data. Most of the data were obtained in the second part of the test and are called series B data.

Data Reduction

The values of skin-friction drag were obtained by subtracting the base drag and forebody pressure-drag coefficients from the total drag coefficient determined by means of the balance. The base drag coefficient was obtained from base-pressure measurements. The forebody pressure drag was determined from measured pressure distributions over the nose of the 85-microinch-roughness model at Reynolds numbers (based on model length) of 7×10^6, 17.5×10^6, and 28×10^6. Since the variation of the value of C_{D_p} with Reynolds number was of about the same order as the scatter in the data, a constant value of $C_{D_p} = 0.101$ was used throughout the Reynolds number range for all the models.

Corrections and Accuracy

No corrections were made for buoyancy since this effect was found to be negligible. Previous calibrations have shown a slight decrease in test-section Mach number at stagnation pressures below 4 lb/sq in. abs. However, estimates indicate that no corrections to the data are required.

The probable error in skin-friction coefficient (based on wetted area) is estimated to be about ± 0.0001 for Reynolds numbers near 15×10^6. At higher Reynolds numbers this value may be conservative, but at the low values of Reynolds number for the configurations with natural transition the error may be two or three times as great.

RESULTS AND DISCUSSION

General Remarks

Sample plots of the types of data obtained in this investigation of surface-roughness effects are shown in figure 3. These curves indicate

the typical variations of total, base, and skin-friction drag coefficients with test Reynolds number that were observed when tests were made without base blocks. The same basic types of data were obtained when base blocks were installed, except that the levels of the total and base drag coefficients were decreased. All coefficients presented here are based on the maximum cross-sectional area of the model. In general, the curves of this figure represent the results of several test runs made on each model. For the 23- and 480-microinch-roughness models, some of the tests were made with considerable time intervening; hence, the tests are identified as series A and series B tests.

With transition fixed, repeat runs were always in good agreement with previous tests. With natural transition, however, considerable difficulty was encountered with sandblast effects such as those depicted by the abrupt rise in the curves for total drag and skin-friction coefficients for the 480-microinch-roughness model at $R = 18 \times 10^6$ or more and the 23-microinch-roughness model at $R = 24 \times 10^6$. Most of the data affected by sandblasting have been omitted; in some instances as many as half a dozen attempts were unsuccessful in obtaining satisfactory results at the higher Reynolds numbers (15×10^6 or more). The results presented in this paper are believed to be the best obtainable from a reasonable attempt at eliminating sandblast effects on aluminum models in this tunnel.

At low Reynolds numbers (below about 15×10^6), the results from the different test runs were in good agreement except that the series A tests on the 23- and 480-microinch-roughness models with natural transition consistently showed a small increase in Reynolds number for transition at the base and a somewhat lower skin-friction coefficient in the lower Reynolds number range relative to the series B tests. The reason for this discrepancy is not known.

Effects of Surface Roughness on Skin Friction

The complete skin-friction results, converted to skin-friction coefficient based on wetted area, are plotted on a logarithmic scale in figure 4. Included in the figure are the theoretical skin-friction curves for the laminar and turbulent boundary layers. The laminar skin-friction curve was computed by the Chapman-Rubesin technique (ref. 4) for a flat plate and converted to a cone-cylinder by means of Mangler's transformation (ref. 5), a zero pressure gradient being assumed. The theoretical turbulent curve was calculated by the extended Frankl-Voishel method of reference 6.

In order to simplify the comparison of the results for the different model roughnesses, the skin-friction data for all four models are presented on a single plot in figure 5. Only data from series B tests are

employed so that the comparison will avoid introducing any effects due
to the aforementioned slight change in skin-friction drag characteris-
tics between the two test series in the lower Reynolds number range
with natural transition. In order to simplify the comparison further,
the test points have been omitted from the curves for natural transition.

The natural-transition results (fig. 5) indicate that at the
lowest test Reynolds numbers the flow over the models is laminar and
the skin-friction drag is approximately parallel to the theoretical
curves, although of somewhat greater magnitude. The difference between
the laminar skin-friction drag coefficients of the various models is
believed to be due largely to the low accuracy resulting from the low
pressures and small forces. At a Reynolds number of 4×10^6 approxi-
mately, transition occurs at the model base and thence begins to move
forward on the body with further increase in Reynolds number. The abrupt
increases in skin friction occurring at the higher Reynolds numbers on
the 23- and 85-microinch-roughness models are attributed mainly to sand-
blasting effects.

A plot of the Reynolds number for transition at the base as a
function of model roughness is presented in figure 6. Since it is
somewhat difficult to determine the transition Reynolds number from the
force tests alone, use was made of the base drag coefficients (fig. 7).
Past experience has indicated that transition at the model base coincides
with the sharp negative-pressure peak or the initial peak in base drag
coefficient. Included in figure 6 is one point from tests of an iden-
tical ogive-cylinder model with a surface roughness of 5 to 6 microinches
root mean square (ref. 7). The results (fig. 6) show a gradual decrease
in transition Reynolds number with increase in model surface roughness.

With transition fixed (fig. 5) the skin-friction drags for the
23- and 85-microinch-roughness models were about equal and in good
agreement with the theoretical skin friction over the Reynolds number
range. It might be noted at this point that the skin-friction drag
results for several NACA RM-10 models (ref. 8) and some ogive-cylinder
and cone-cylinder models (ref. 7) having the same fineness ratio and a
surface roughness of about 5 to 6 microinches root mean square are in
good agreement with one another and with the extended Frankl-Voishel
theoretical curve at this Mach number. Thus, it may be concluded that
this theory is representative of the skin-friction results obtained in
the Langley 4- by 4-foot supersonic pressure tunnel at $M = 1.61$ and
that, for bodies of high fineness ratio, body shapes and pressure gradi-
ents have little effect on the average turbulent skin-friction drag
coefficients.

As the surface roughness is increased from 85 to 240 and 480 micro-
inches root mean square, the skin-friction curves for the rougher models
first follow the skin-friction curves for the smoother bodies and then

begin to diverge (fig. 5). For the 480-microinch-roughness model, the divergence Reynolds number was estimated to be about 7×10^6 and for the 240-microinch-roughness model about 17×10^6. The fact that the skin-friction coefficients are still increasing with Reynolds number at the highest test Reynolds number for the 480-microinch-roughness model indicates that the surface friction has not yet reached the point where it is independent of Reynolds number and becomes a function of roughness height only (ref. 1). It might be expected that the skin-friction coefficients for the 240-microinch-roughness model will also increase somewhat at Reynolds numbers larger than those of the tests before leveling off in the region where skin friction is independent of Reynolds number.

In these tests the largest increment in skin-friction drag was measured on the 480-microinch-roughness model at the highest test Reynolds number of 37×10^6. This increment was about 60 percent of the skin-friction drag of the smooth body with turbulent boundary layer at that value of Reynolds number. At higher Reynolds numbers, of course, the increment in terms of smooth-body drag would increase still further.

The relatively high drag for the 480-microinch-roughness model (fig. 5) in the Reynolds number range from 3×10^6 to 6×10^6 may be partly due to the wave drag of the roughness at the forward end of the distributed roughness. The decrease in skin friction for the same model at the lowest values of Reynolds number apparently occurred because the transition strip was not made sufficiently rough to fix transition when the laminar boundary layer was relatively thick. The roughness of the transition strip is dependent upon the depth to which the carborundum grains are imbedded in the lacquer adhesive and this depth is difficult to control.

Comparison With Nikuradse's Results

The Reynolds numbers at which surface roughness first caused an increase in skin-friction drag above that for a smooth body with turbulent flow are compared with Nikuradse's results reduced to a flat plate (ref. 2) in figure 8. The plots are made as functions of both Reynolds number and Reynolds number per foot for reasons that will be apparent from subsequent discussions. The curves may also be interpreted as depicting the allowable roughness height at any R or R_{ft} below which there will be no effects due to roughness. In order to effect this comparison it was assumed that the surface roughness on the present test models was approximately sinusoidal in nature and that the root-mean-square values could be converted to maximum height by dividing by 0.707. The Nikuradse curve was obtained by plotting values of divergence Reynolds number for a flat plate as indicated by references 2 or 9 as a function of roughness parameter k'/L and fairing an average curve through the points.

The agreement between the present results for the 480- and 240-microinch-roughness models and Nikuradse's data is good. This agreement may be fortuitous because of a possible error in the roughness conversion factor, the different types of surface roughness used in the investigations (circumferential ridges and sand grains), and the fact that three-dimensional boundary-layer flow occurs on the ogive-cylinder and two-dimensional boundary-layer flow on the flat plate. For these reasons it would be inappropriate to conclude that there is no effect of Mach number on divergence Reynolds number within the Mach number range under consideration, from 0 to 1.61.

The allowable roughness represented by the curve in figure 8(a) can be expressed by the equation

$$\left(\frac{UL}{\nu}\right)^{0.9} \frac{k'_{ad}}{L} = 19.8 \tag{1}$$

or

$$k'_{ad} = 19.8L^{0.1}R_{ft}^{-0.9} \tag{2}$$

Thus, it appears that the allowable roughness height is essentially independent of model length and dependent primarily upon changes in Reynolds number per foot. The appearance of the length parameter stems from the use of Nikuradse's data and is believed to result fortuitously from the choice of variables involved in presenting Nikuradse's data in terms of flat-plate variables. It appears unrealistic that an increase in model length should result in an increase in allowable roughness height when nothing else is changed. From figure 8(b) an equation can be derived which does not involve L and which is probably just as accurate. This equation, in terms of k_{ad}, is

$$k_{ad} = 19.8R_{ft}^{-0.9} \tag{3}$$

An interesting insight as to the permissible surface roughness at supersonic speeds can be obtained from equation (3) or the curve of figure 8(b). For example, it is found that, for an airplane or missile flying at the test Mach number at an altitude of 50,000 feet, the allowable surface roughness is 660 microinches or about 470 microinches root mean square. If the flight takes place at sea level the allowable roughness is reduced to 130 microinches or about 90 microinches root mean square. If the same relationship found in the present tests and

in Nikuradse's tests should hold to higher Mach numbers, then at M = 5
the allowable surface roughnesses at 50,000 feet and at sea level would
become about 160 and 30 microinches root mean square, respectively.
Apparently, then, surface-roughness effects are most critical at low
altitudes and at high speeds.

The variation of the incremental drag due to surface roughness ΔC_{f_w}
with change in R or R_{ft} is shown in figure 9. The results are again
compared with Nikuradse's data reduced to a flat plate (ref. 2) and
again the agreement is good, except that the present results for the
480-microinch-roughness model apparently increase somewhat more rapidly
with Reynolds number than do the results from reference 1. This more
rapid increase in ΔC_{f_w} with R in the present tests may be due to
the appearance of an increasing amount of wave drag as the roughness
protrudes farther into the supersonic portion of the boundary layer as
the boundary layer becomes thinner at the higher tunnel pressures.
Nevertheless, it may be broadly concluded that the effects of surface
roughness for a turbulent boundary layer at supersonic speeds are very
similar to those at subsonic speeds.

It should be noted here that, although the divergence Reynolds number
in these tests is dependent almost exclusively on free-stream Reynolds
number and hence only on the free-stream flow conditions, the increment
in skin-friction drag due to surface roughness is dependent upon the
boundary-layer thickness within the Reynolds number range under considera-
tion in figure 7. Therefore, since the turbulent boundary layer is
thinnest immediately behind the transition region, for the tests with
natural transition the first appearance and the largest increment in local
skin-friction drag due to roughness will probably occur in this region.

When the turbulent boundary layer is sufficiently thin, of course,
as at extremely high Reynolds numbers, the increment in skin friction
due to roughness no longer depends upon Reynolds number but depends
solely upon the average roughness height (refs. 1 and 2) as noted
previously.

Effects of Roughness Location

In reference 10, Von Kármán notes that Nikuradse's results indicate
that the first appearance of drag due to surface roughness always occurs
when the surface roughness begins to exceed one-fourth the height of the
laminar sublayer. Consequently, it may be expected that an increase in
divergence Reynolds number should be noted if the surface roughness does
not cover the whole body but begins some distance behind the nose of the

body. The results of tests made to determine the accuracy of this prodiction are shown in figure 10. The data indicate that there was no change in divergence Reynolds number when either the forward half or the rear half of the cylinder of the essentially smooth (23-microinchroughness) model was covered with sandpaper.

In order to study the problem further, the thickness of the laminar sublayer over the length of the model was computed for several values of R, a 1/7-power profile in incompressible flow being assumed. The results are presented in figure 11. The plot indicates that the change in δ_L along the body is relatively small, particularly at the higher values of R, and the major change in sublayer thickness occurs as a result of changes in pressure or Reynolds number per foot. An estimate from the curves of figure 11 shows that a change in divergence Reynolds number of the order of 10 percent, or within the accuracy of the tests, should be expected for the two roughness locations. Hence, no reliable conclusion regarding the effects of laminar-sublayer thickness can be made.

Temperature-Recovery Characteristics

The variation of temperature-recovery factor with x/L for the 23- and 480-microinch-roughness models at several values of Reynolds number is presented in figure 12. For fixed transition the recovery factors of the two models are essentially the same within the accuracy of the measurements and appear to be about constant through the Reynolds number range investigated. The results of the tests with natural transition indicate no significant differences in recovery factor for the two models in the laminar-flow region. Small changes appear in the Reynolds number region where transition is at a different location on each model. Average values of recovery factor on the cylindrical afterbody were about 0.87 and 0.90 for laminar and turbulent boundary layers, respectively.

SUMMARY OF RESULTS

An investigation has been made of the effects of distributed surface roughness on the skin-friction drag of an ogive-cylinder body of revolution at a Mach number of 1.61. The tests were made at zero angle of attack over a roughness range from 23 to 480 microinches root mean square and over a Reynolds number range from 2.5×10^6 to 37×10^6 based on body length. The results indicate that:

1. The effects of surface roughness at a Mach number of 1.61 are generally similar to those found at subsonic speeds.

2. Both the allowable roughness height for a turbulent boundary layer and the variation with Reynolds number of the increment in skin-friction drag due to roughness are in good agreement with Nikuradse's low-speed results. The agreement may be somewhat fortuitous, however, because of the different types of surface roughness employed and because of the comparison between a three-dimensional body and a flat plate.

3. At constant speed, the allowable roughness height is nearly independent of model length and dependent primarily upon changes in ambient static pressure or Reynolds number per foot. As an approximation, in inches root mean square,

Allowable roughness height = $19.8 \times$ (Reynolds number per foot)$^{-0.9}$

4. An increase in surface roughness caused a small decrease in the Reynolds number for transition at the model base.

5. Surface roughness had little or no effect on surface-temperature-recovery factors for the laminar or turbulent boundary layers; the temperature-recovery factors on the cylindrical portion of the model were about 0.87 and 0.90 for the laminar and turbulent boundary layers, respectively.

6. Pressure gradients or body shapes apparently have little or no effect on the average skin-friction drag coefficient for smooth bodies of high fineness ratio when the boundary layer is turbulent.

Langley Aeronautical Laboratory,
    National Advisory Committee for Aeronautics,
        Langley Field, Va., January 11, 1954.

REFERENCES

1. Nikuradse, J.: Laws of Flow in Rough Pipes. NACA TM 1292, 1950.

2. Prandtl, L., and Schlichting, H.: Das Widerstandsgesetz rauher
   Platten. Werft Reederei Hafen, Jahrg. 15, Heft 1, Jan. 1, 1934,
   pp. 1-4.

3. Czarnecki, K. R., and Sinclair, Archibald R.: Preliminary Investiga-
   tion of the Effects of Heat Transfer on Boundary-Layer Transition
   on a Parabolic Body of Revolution (NACA RM-10) at a Mach Number
   of 1.61. NACA TN 3165, 1954. (Supersedes NACA RM L52E29a.)

4. Chapman, Dean R., and Rubesin, Morris W.: Temperature and Velocity
   Profiles in the Compressible Laminar Boundary Layer With Arbitrary
   Distribution of Surface Temperature. Jour. Aero. Sci., vol. 16,
   no. 9, Sept. 1949, pp. 547-565.

5. Mangler, W.: Boundary Layers With Symmetrical Airflow About Bodies
   of Revolution. Rep. No. R-30-18, Part 20, Goodyear Aircraft Corp.,
   Mar. 6, 1946.

6. Rubesin, Morris W., Maydew, Randall C., and Varga, Steven A.: An
   Analytical and Experimental Investigation of the Skin Friction of
   the Turbulent Boundary Layer on a Flat Plate at Supersonic Speeds.
   NACA TN 2305, 1951.

7. Hilton, John H., Jr., and Czarnecki, K. R.: An Exploratory Investi-
   gation of Skin Friction and Transition on Three Bodies of Revolution
   at a Mach Number of 1.61. NACA TN 3193, 1954.

8. Czarnecki, K. R., and Sinclair, Archibald R.: An Extension of the
   Investigation of the Effects of Heat Transfer on Boundary-Layer
   Transition on a Parabolic Body of Revolution (NACA RM-10) at a
   Mach Number of 1.61. NACA TN 3166, 1954. (Supersedes NACA RM L53B25.)

9. Schlichting, H.: Lecture Series "Boundary Layer Theory." Part II -
   Turbulent Flows. NACA TM 1218, 1949.

10. Von Kármán, Th.: Turbulence and Skin Friction. Jour. Aero. Sci.
    vol. 1, no. 1, Jan. 1934, pp. 1-20.

TABLE 1

DIMENSIONS OF MODELS

L, in.	d, in.	k, μin. rms	S_f, ft^2	S_w, ft^2
50.0	4.03	23 ± 5	0.0886	4.05
50.0	4.05	85 ± 15	.0895	4.07
50.1	4.06	240 ± 60	.0899	4.08
49.9	4.08	480 ± 50	.0908	4.09

TABLE 2

LOCATION OF THERMOCOUPLES ON MODELS

Thermocouple number (a)	x, in	x/L
1, 16	3.05	0.06
2	6.01	.12
3	8.05	.16
4	11.02	.22
5	13.07	.26
6, 17	15.03	.30
7	18.03	.36
8	21.03	.42
9, 18	24.04	.48
10	26.08	.52
11, 19	29.04	.58
12	33.04	.66
13	37.04	.74
14, 20	44.06	.88
15	48.03	.96

[a]Thermocouples 1 to 15 on top of model; 16 to 20 on bottom.

CONFIDENTIAL
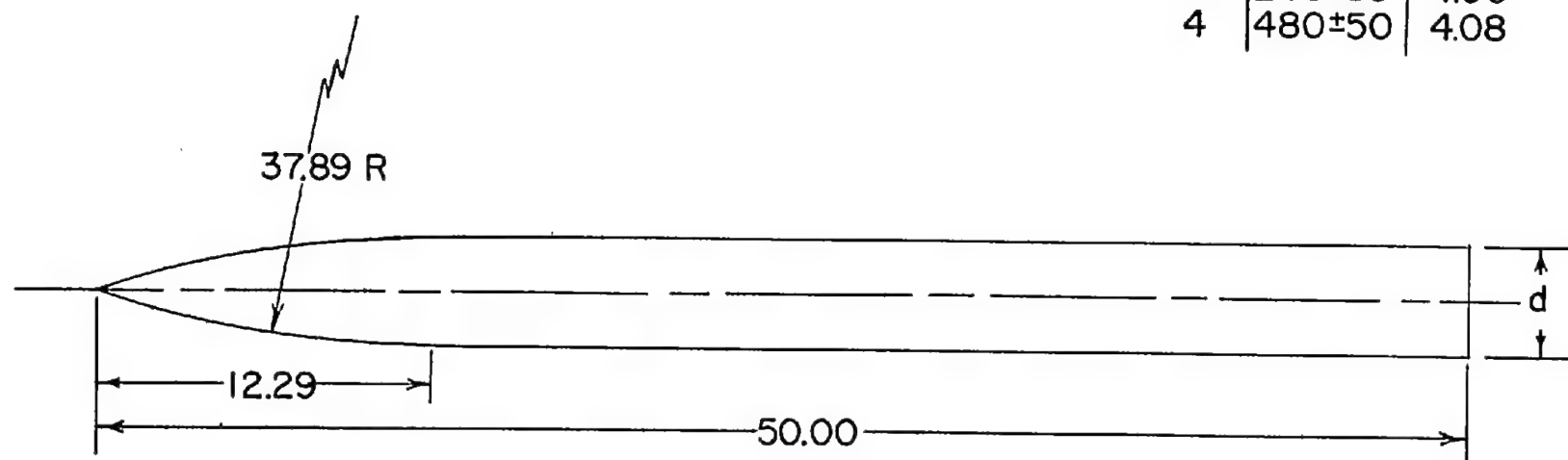
Model	k	d
1	23±5	4.03
2	85±15	4.05
3	240±60	4.06
4	480±50	4.08

37.89 R

12.29

50.00

d

Figure 1.- Drawing of test model. All dimensions are in inches except as noted. k is rms roughness in microinches.
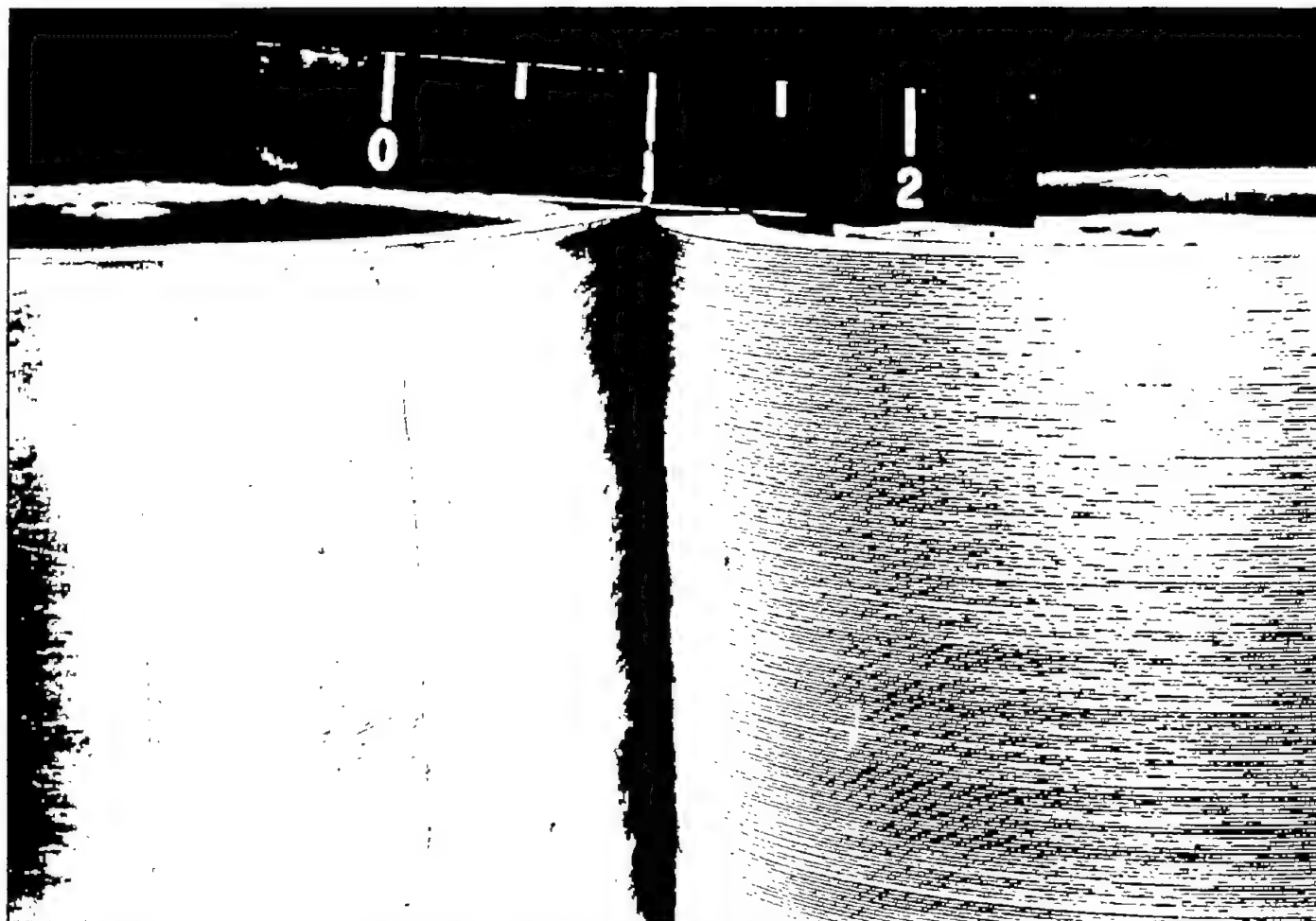
L-82581

23 microinches   480 microinches

Figure 2.- Details of surfaces of 23- and 480-microinch-roughness models.
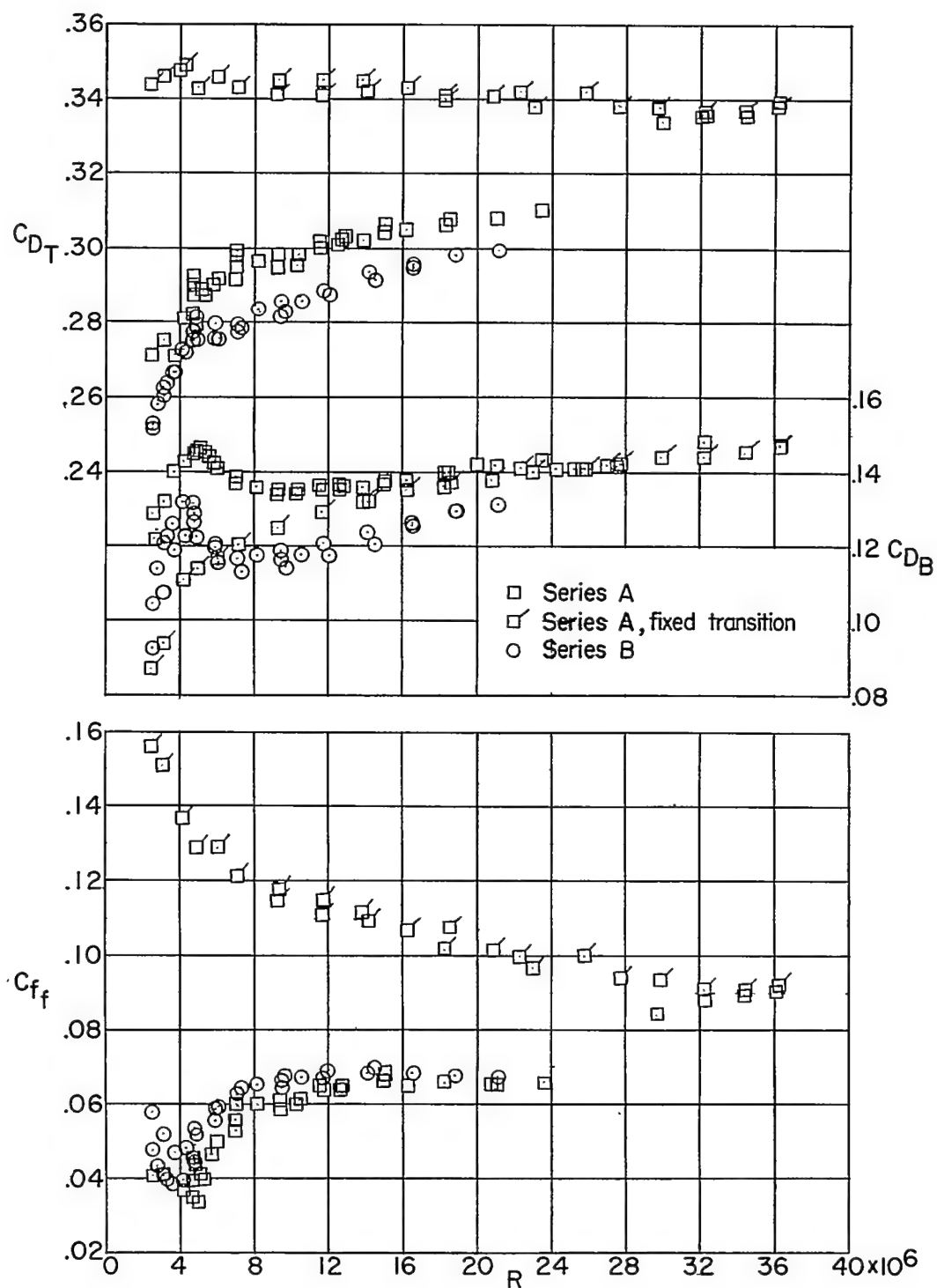
(a) 23 microinches.

Figure 3.- Representative variation of C_{D_T}, C_{D_B}, and C_{f_f} with Reynolds number.
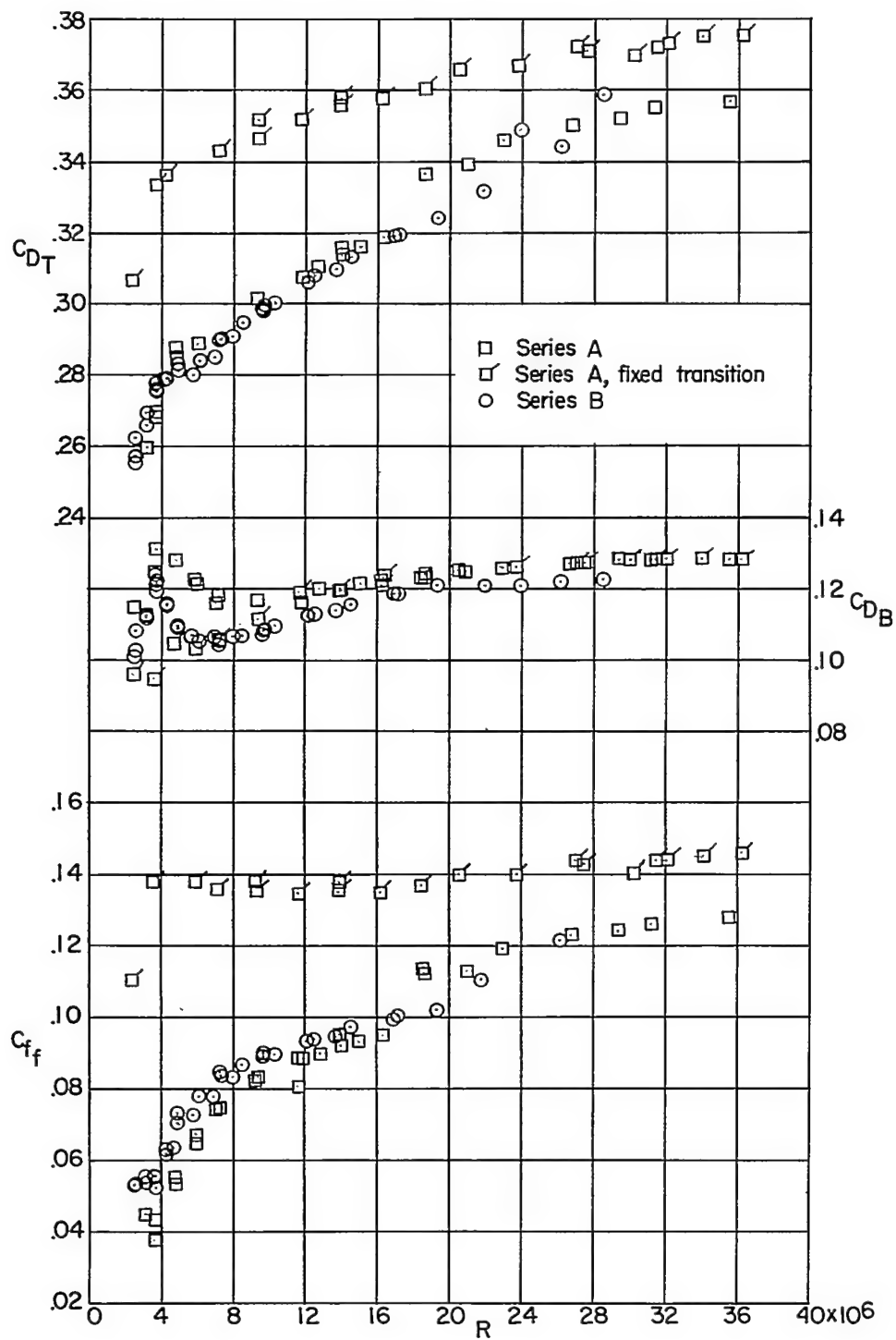
(b) 480 microinches.

Figure 3.- Concluded.
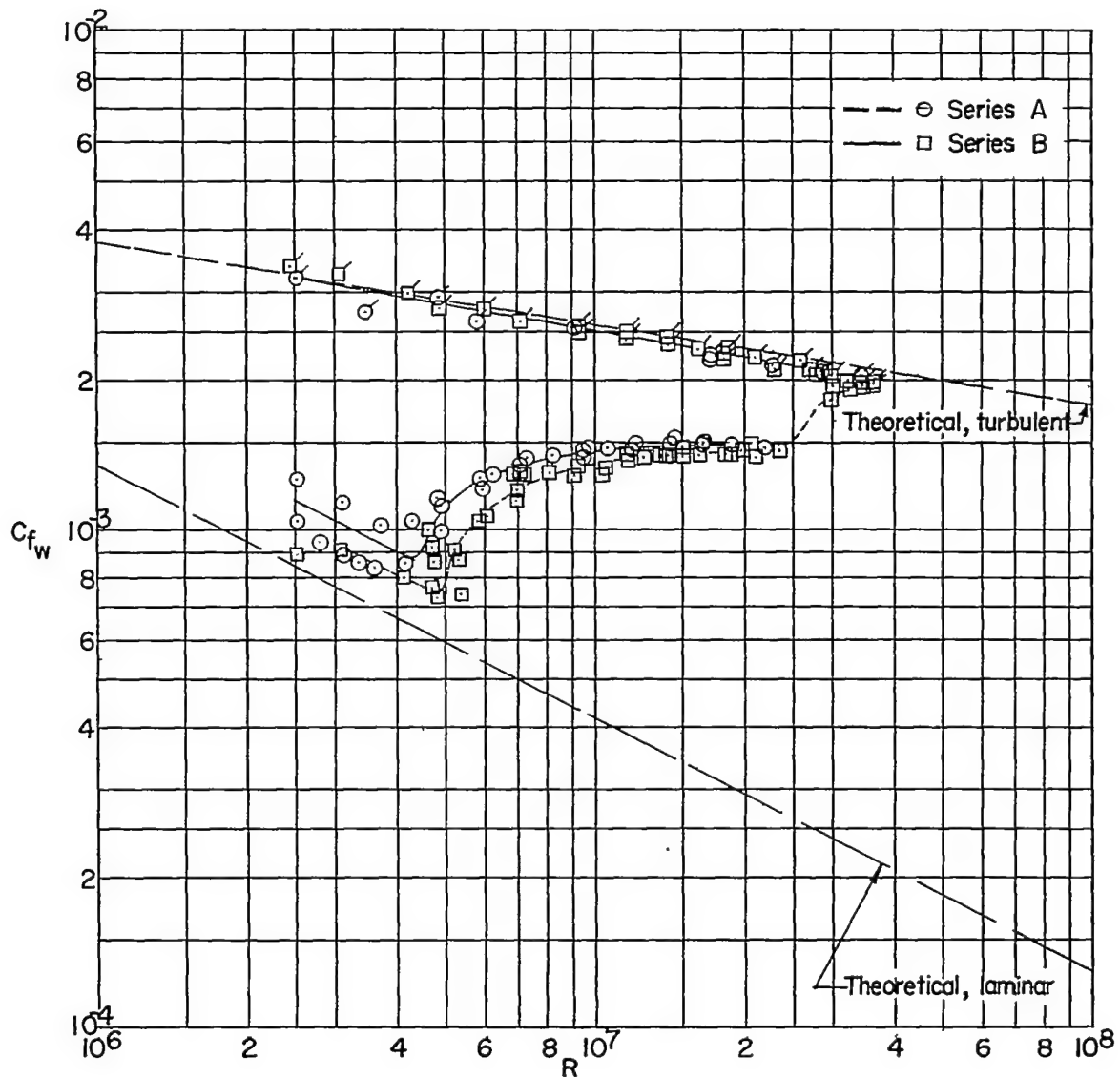
(a) 23 microinches.

Figure 4.- Variation of C_{f_w} with R for several values of surface roughness. Flagged symbols indicate fixed transition.
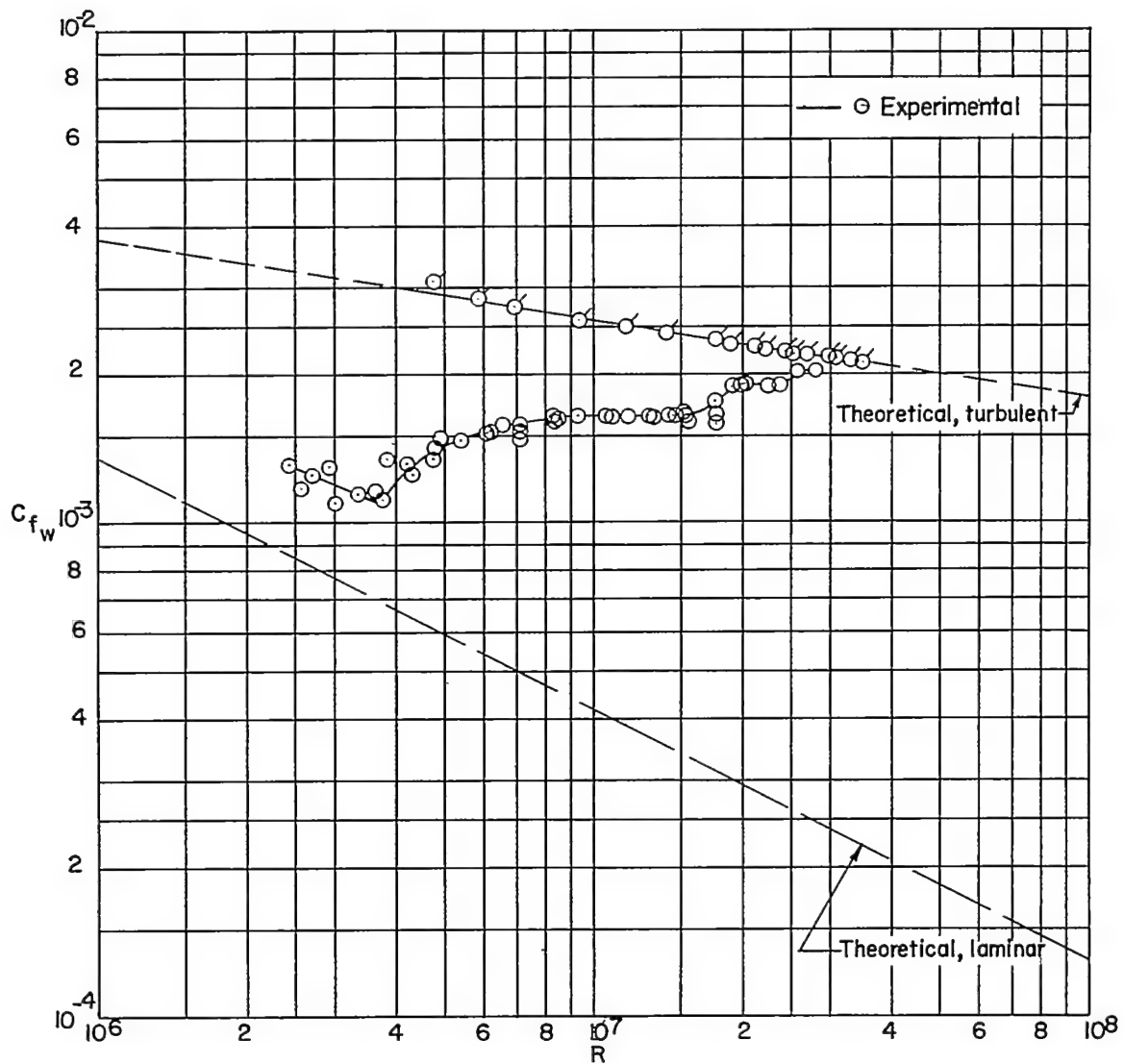
(b) 85 microinches.

Figure 4.- Continued.
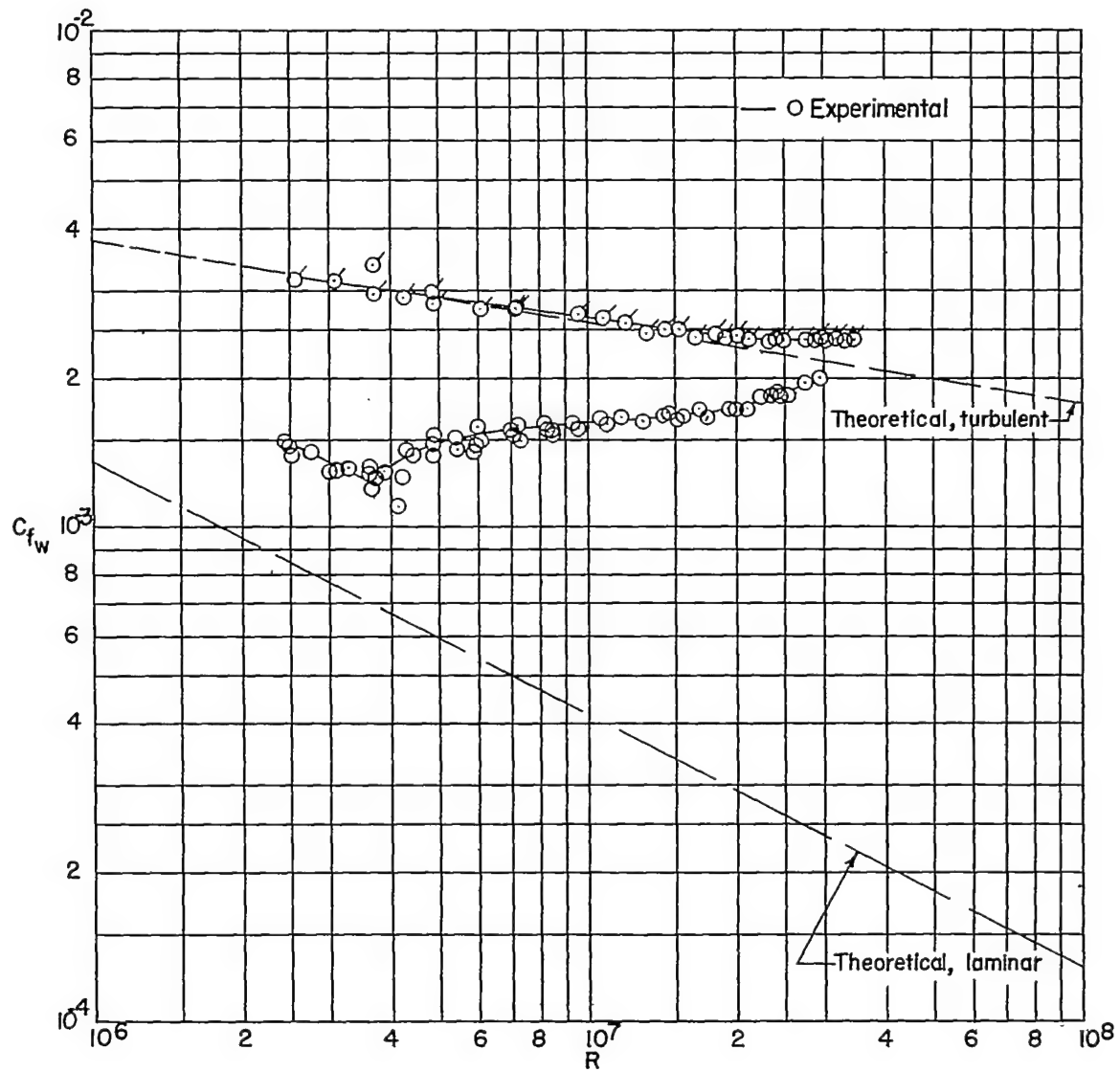
(c) 240 microinches.

Figure 4.- Continued.
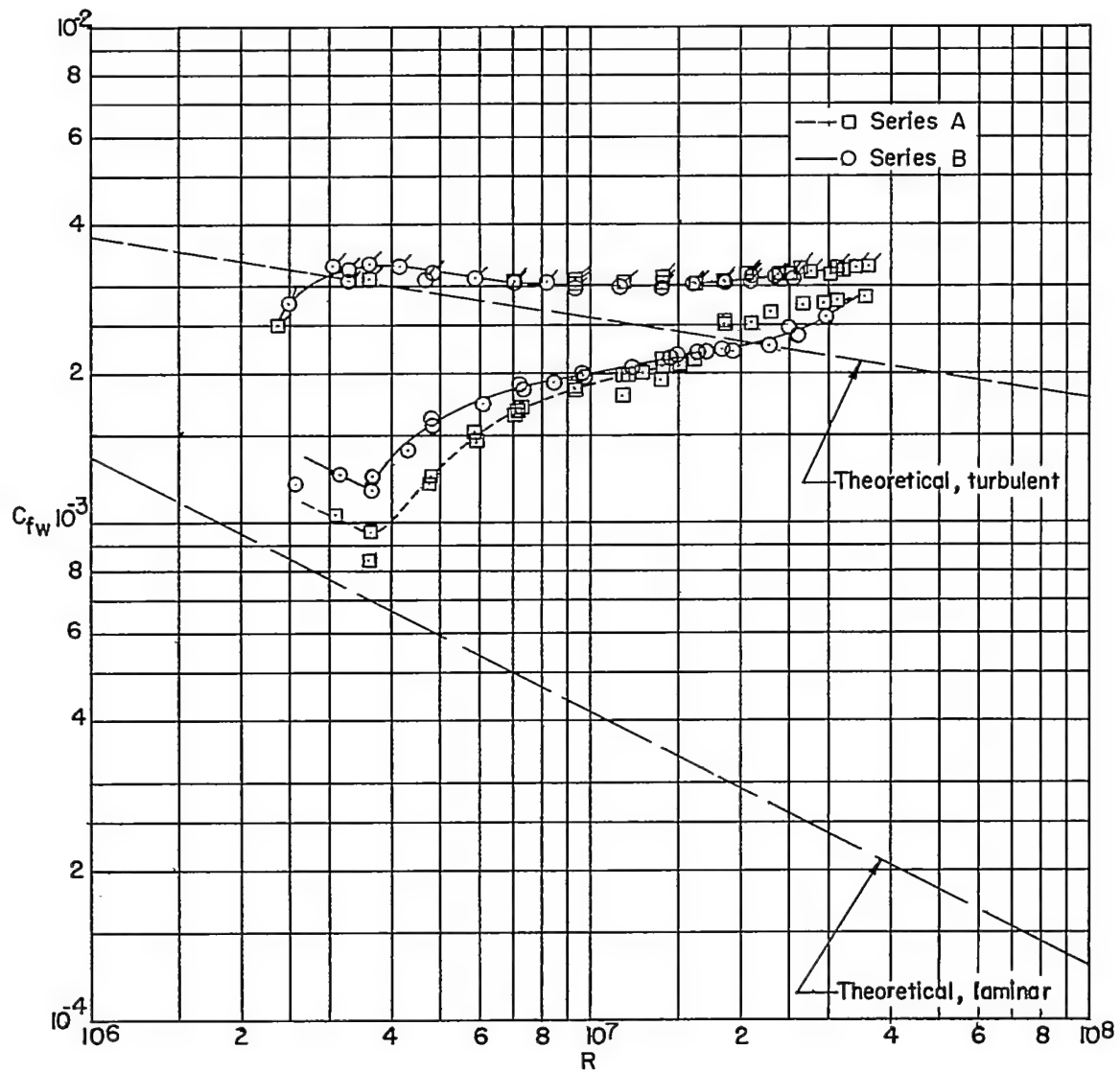
(d) 480 microinches.

Figure 4.- Concluded.
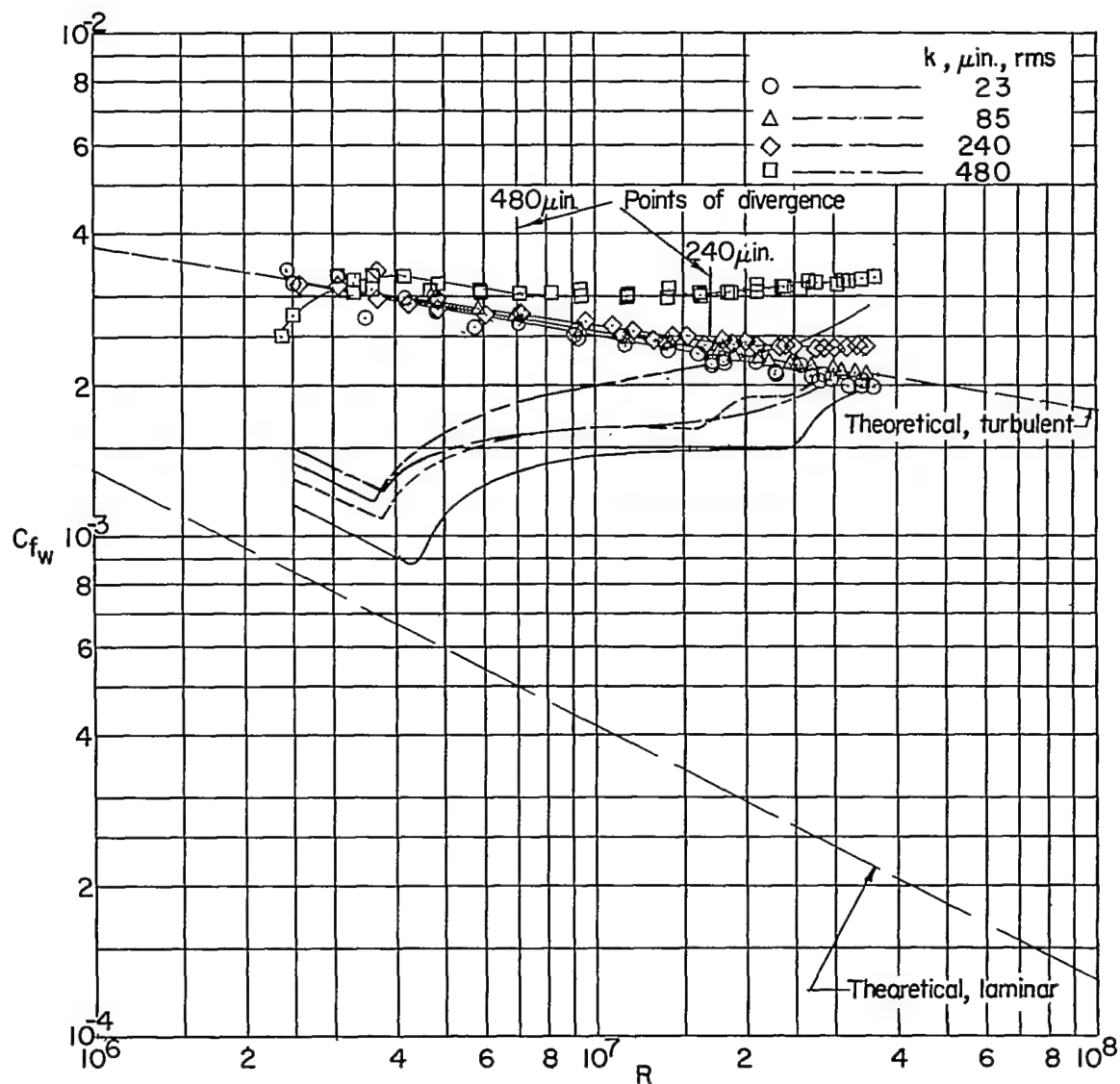
Figure 5.- Summary of results of surface-roughness effects.
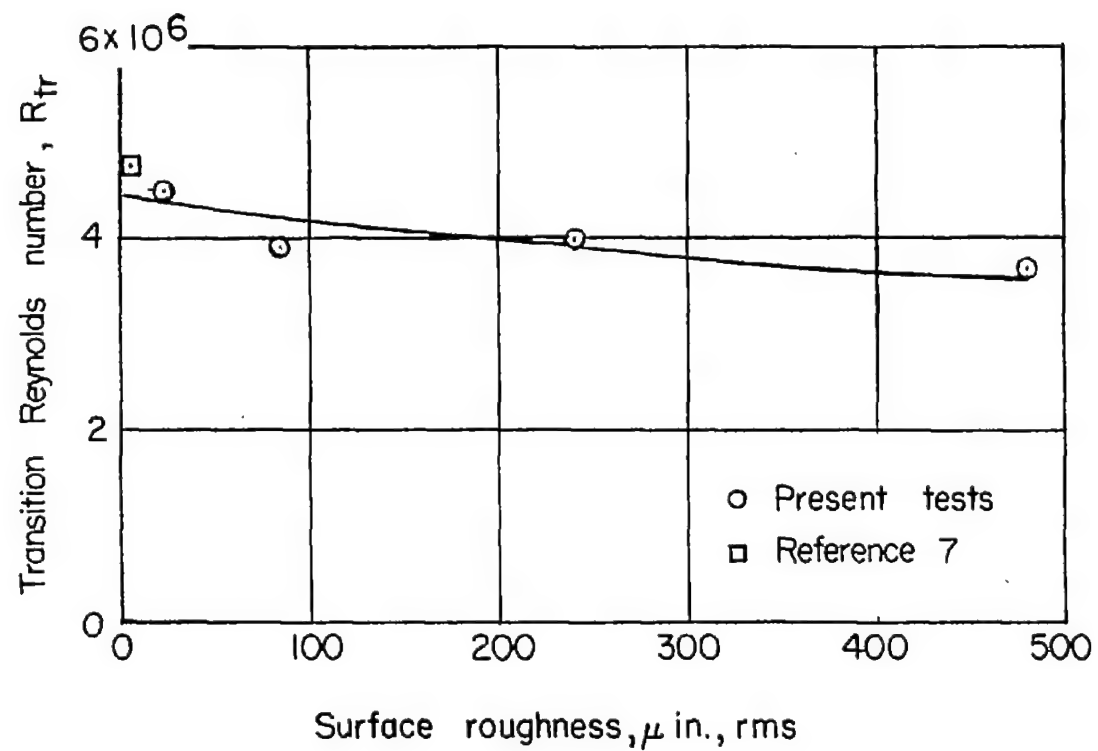
Figure 6.- Variation of R_{tr} with surface roughness.
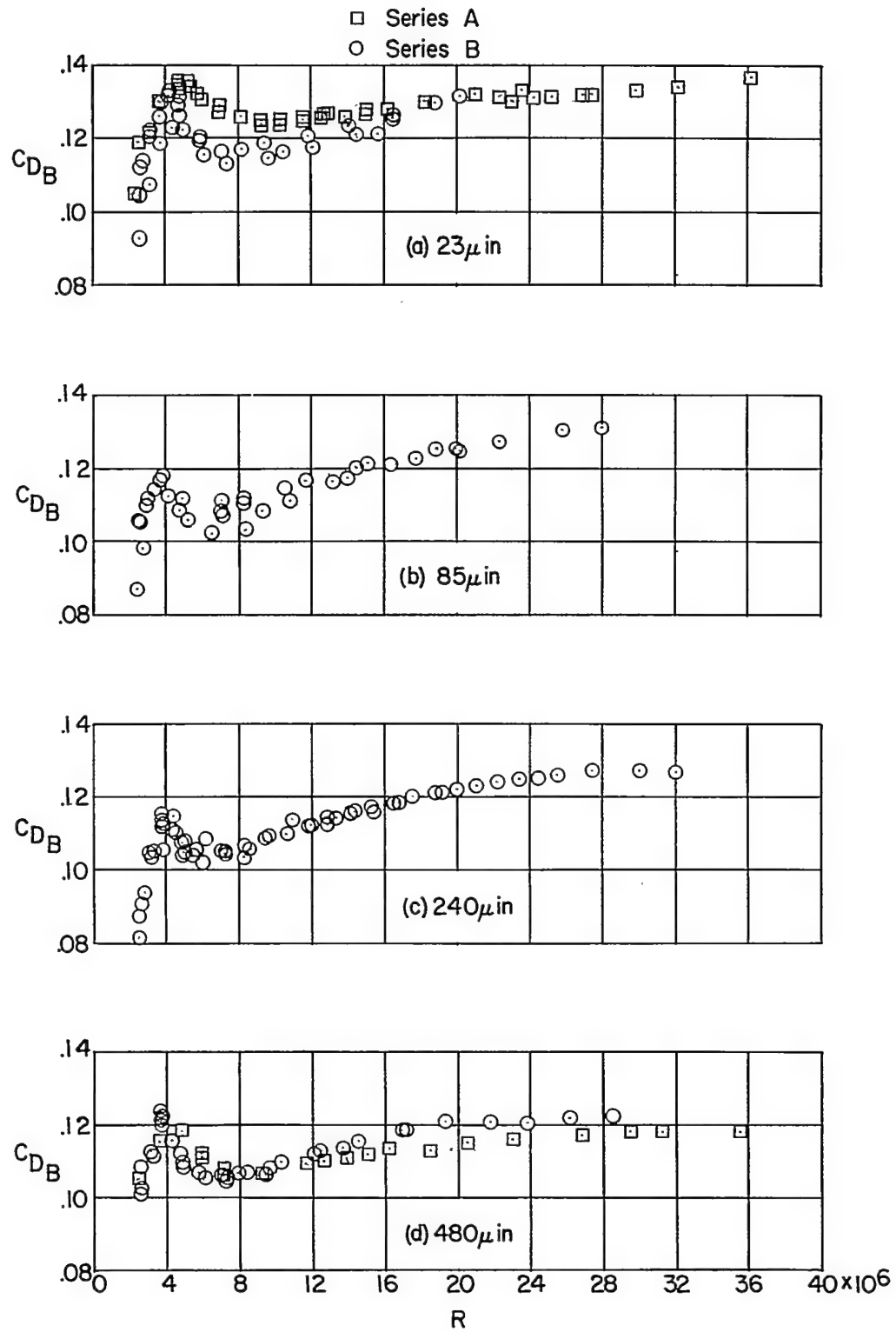
Figure 7.- Variation of base drag coefficient with Reynolds number.
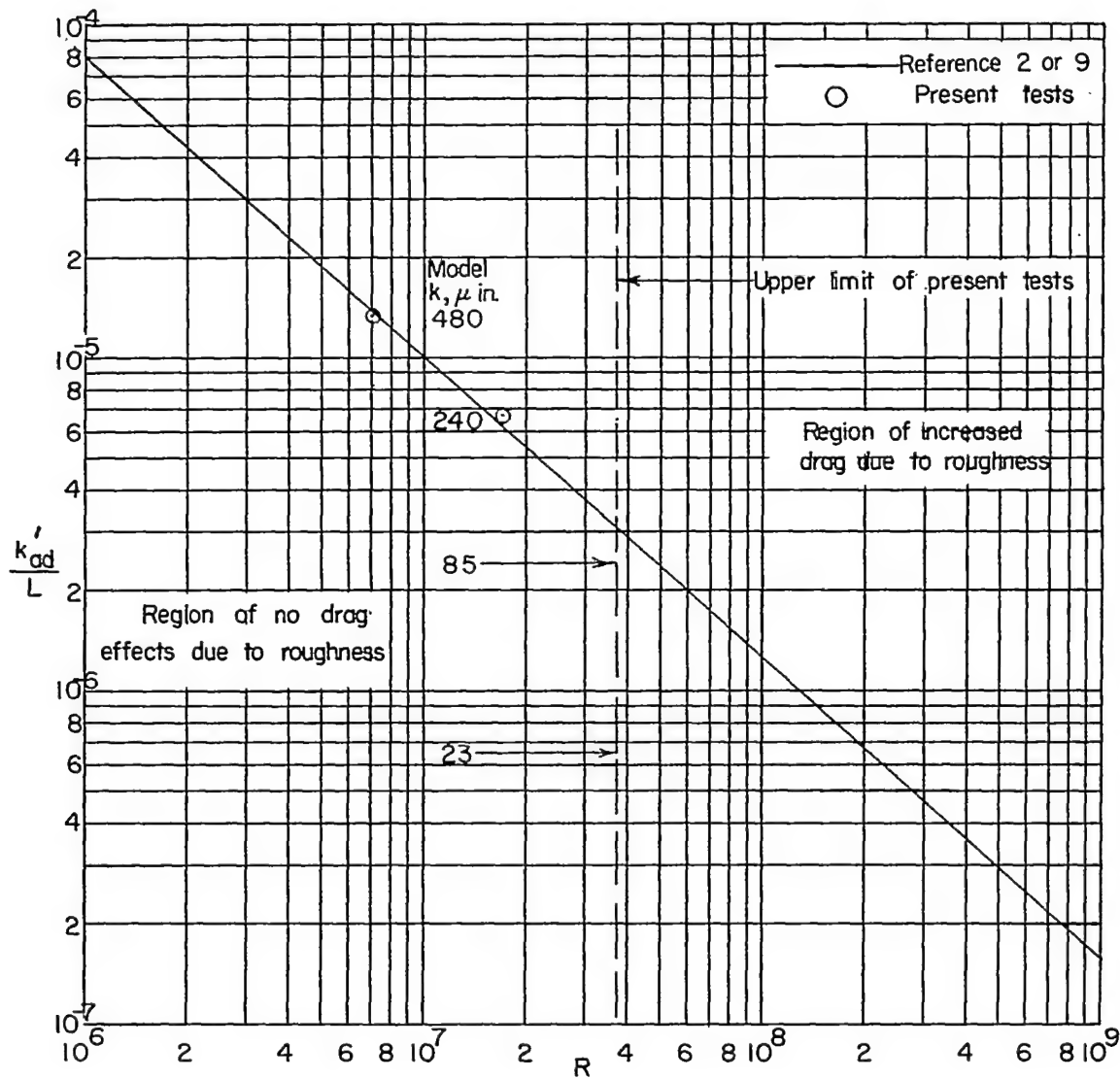
(a) k'_{ad}/L as a function of R.

Figure 8.- Comparison of allowable-roughness results for ogive-cylinder
and flat plate.
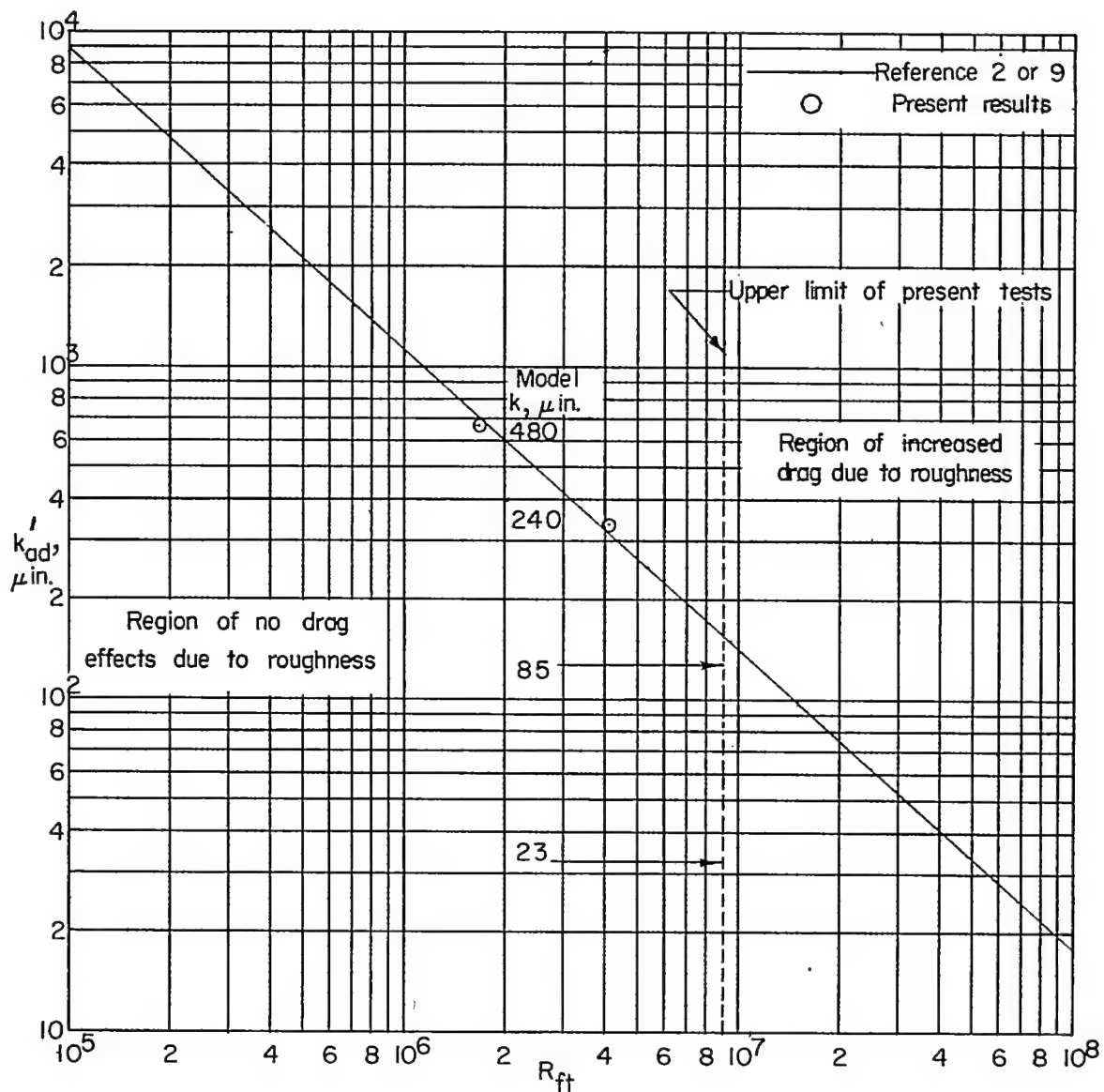
(b) k'_{ad} as a function of R_{ft}.

Figure 8.- Concluded.
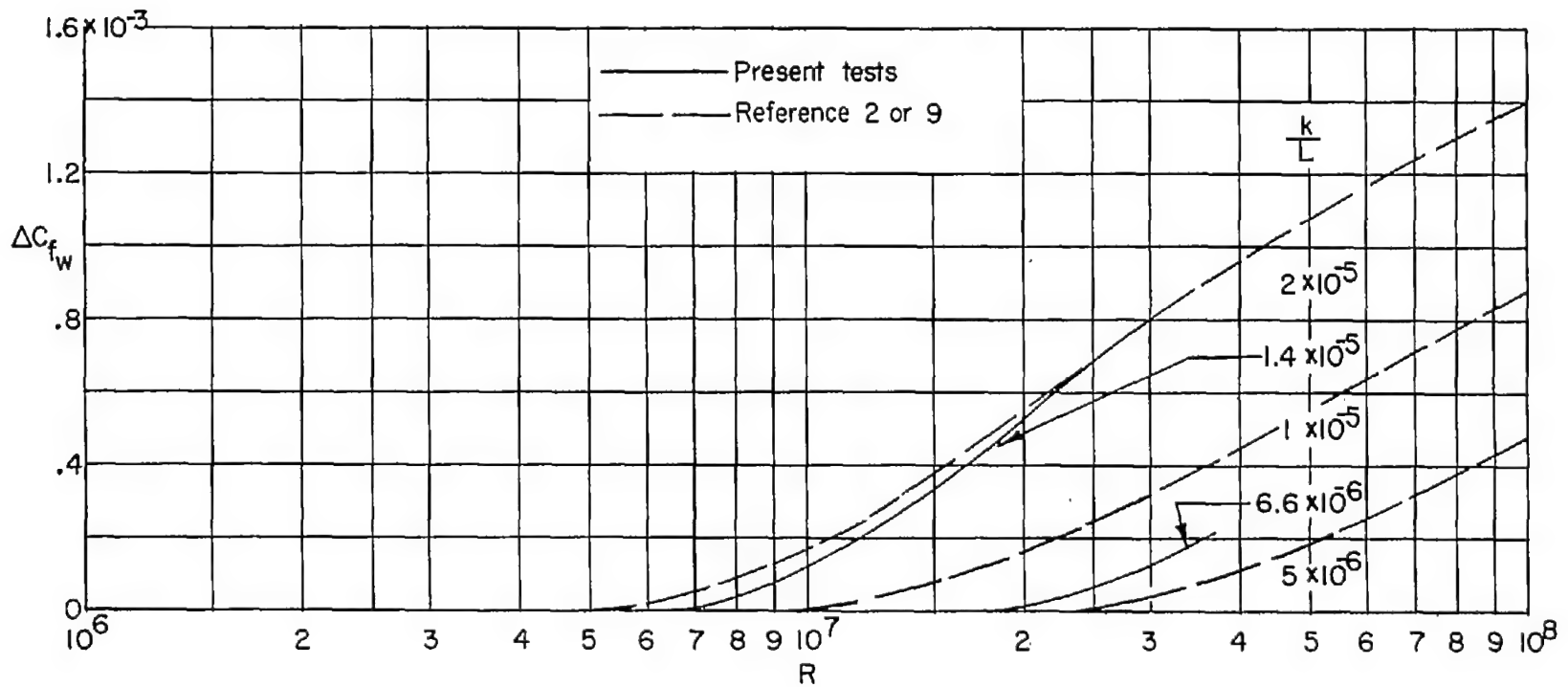
(a) ΔC_{f_W} as a function of R.

Figure 9.- Variation of ΔC_{f_W} with Reynolds number for various values of k'.
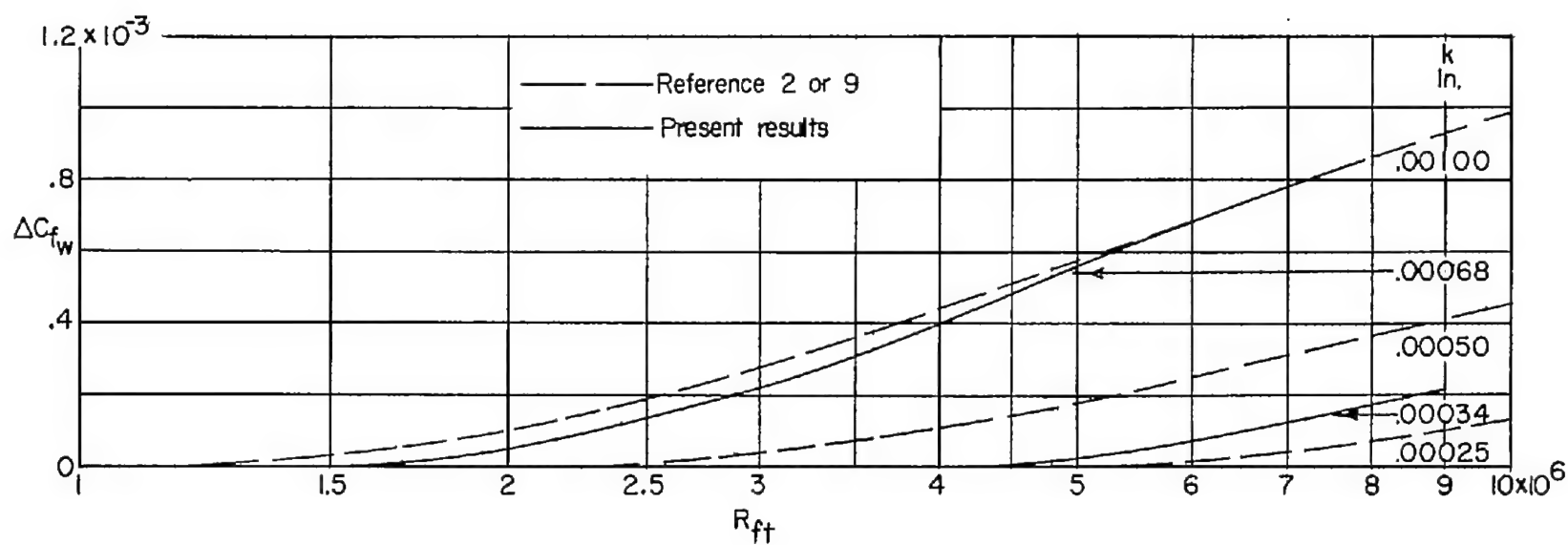
(b) ΔC_{f_W} as a function of R_{ft}.

Figure 9.- Concluded.
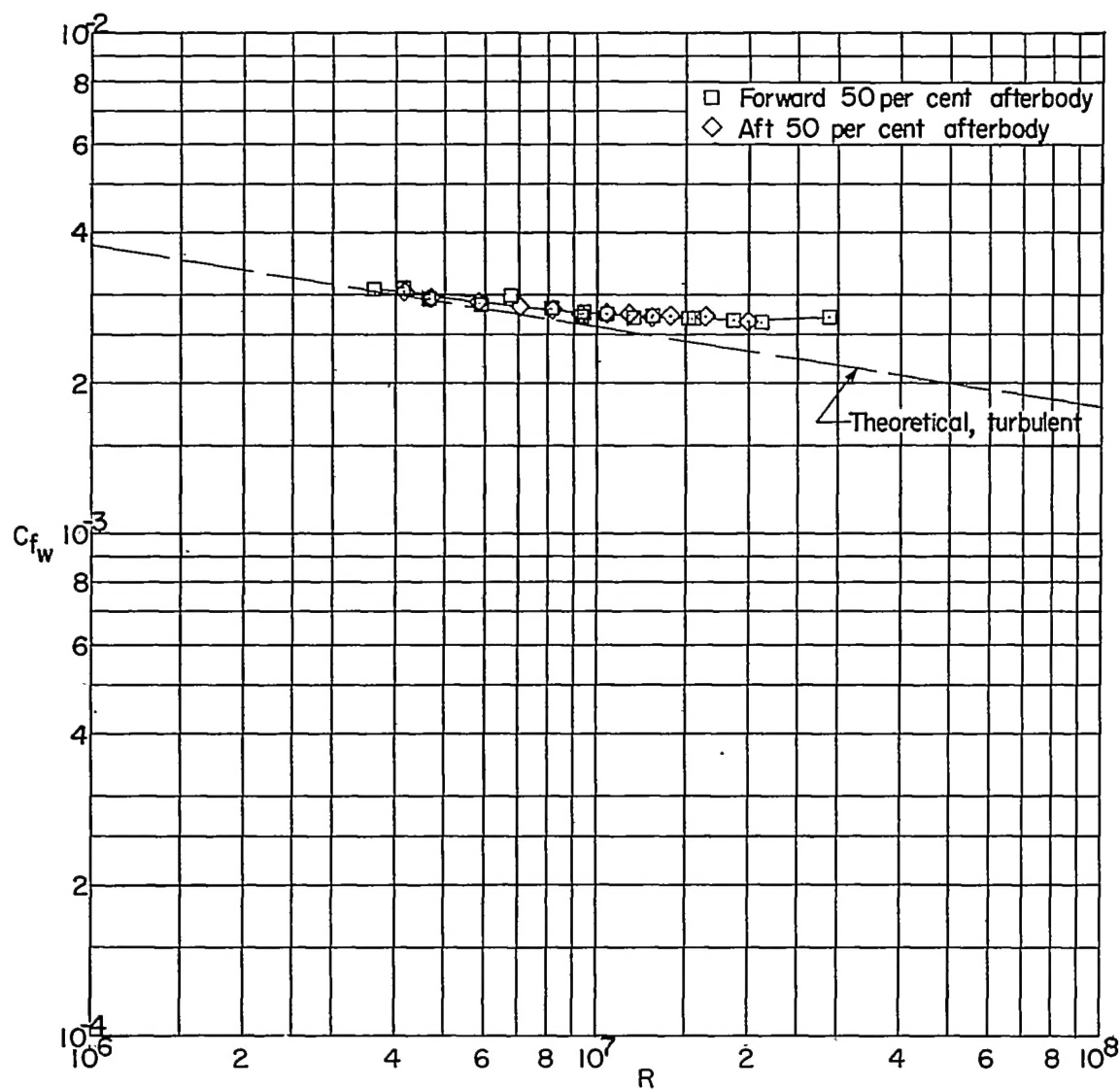
Figure 10.- Effect of adding sandpaper (k ≈ 450 ± 50 microinches root-
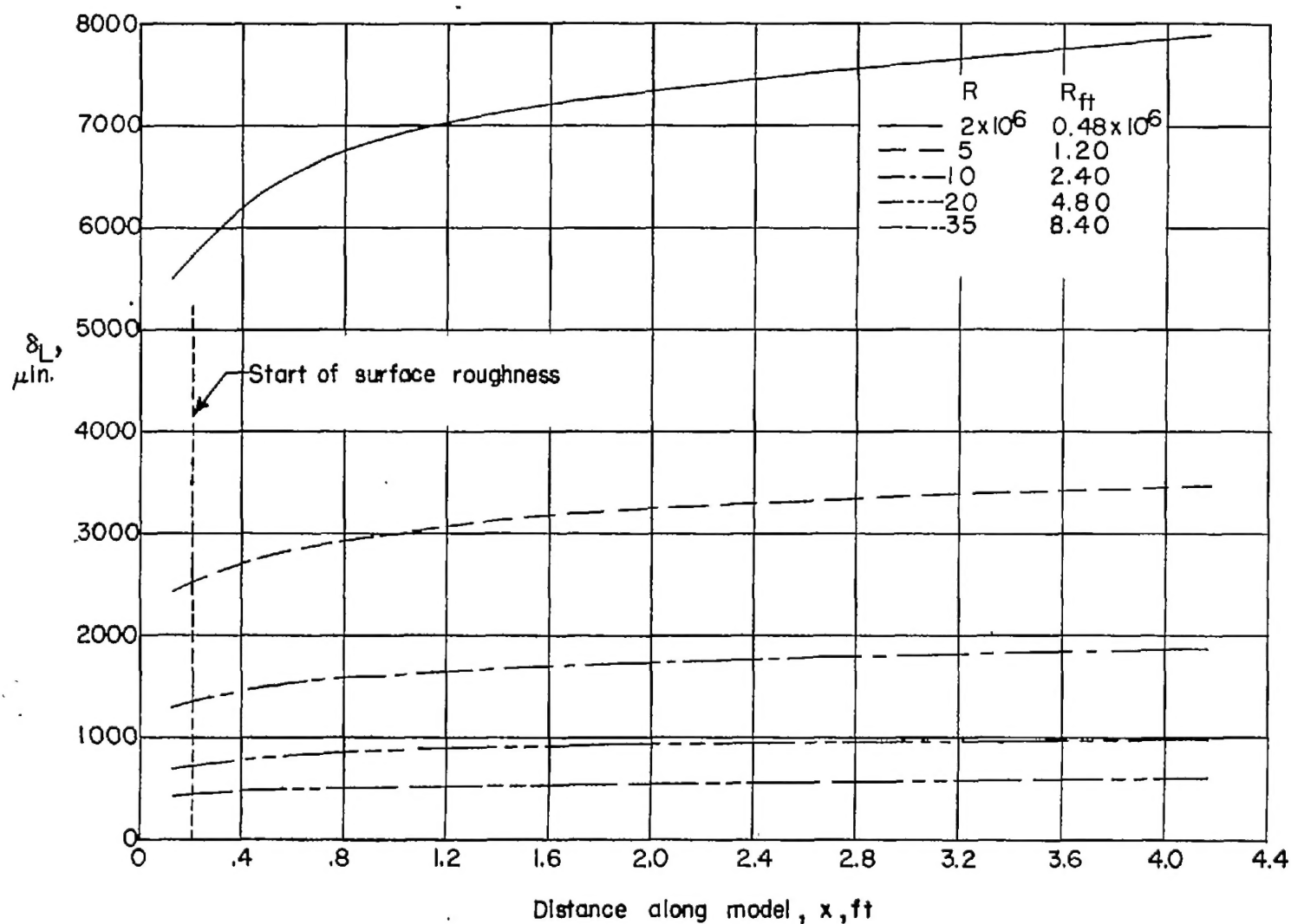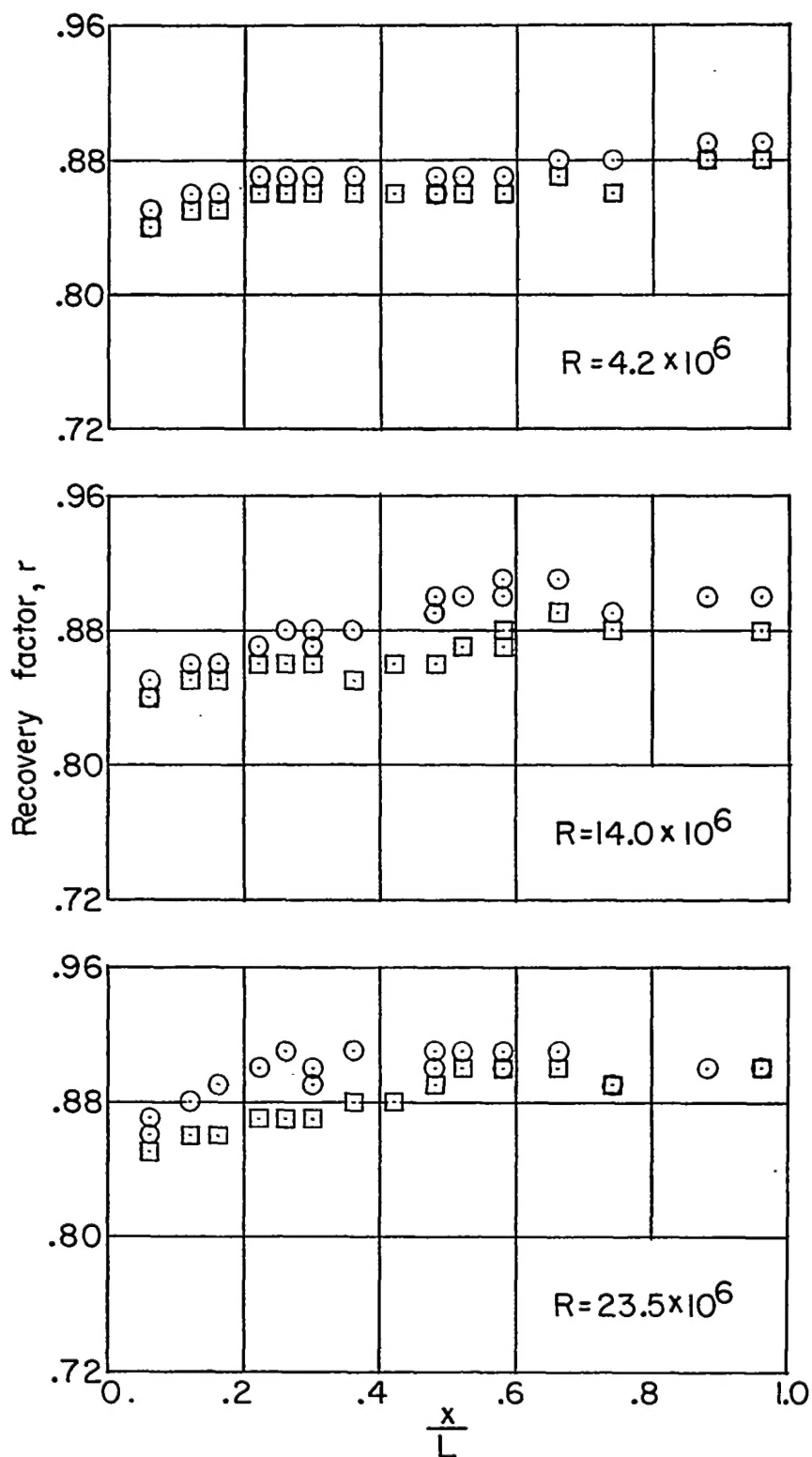mean-square) to cylindrical afterbody of 23-microinch-roughness model.
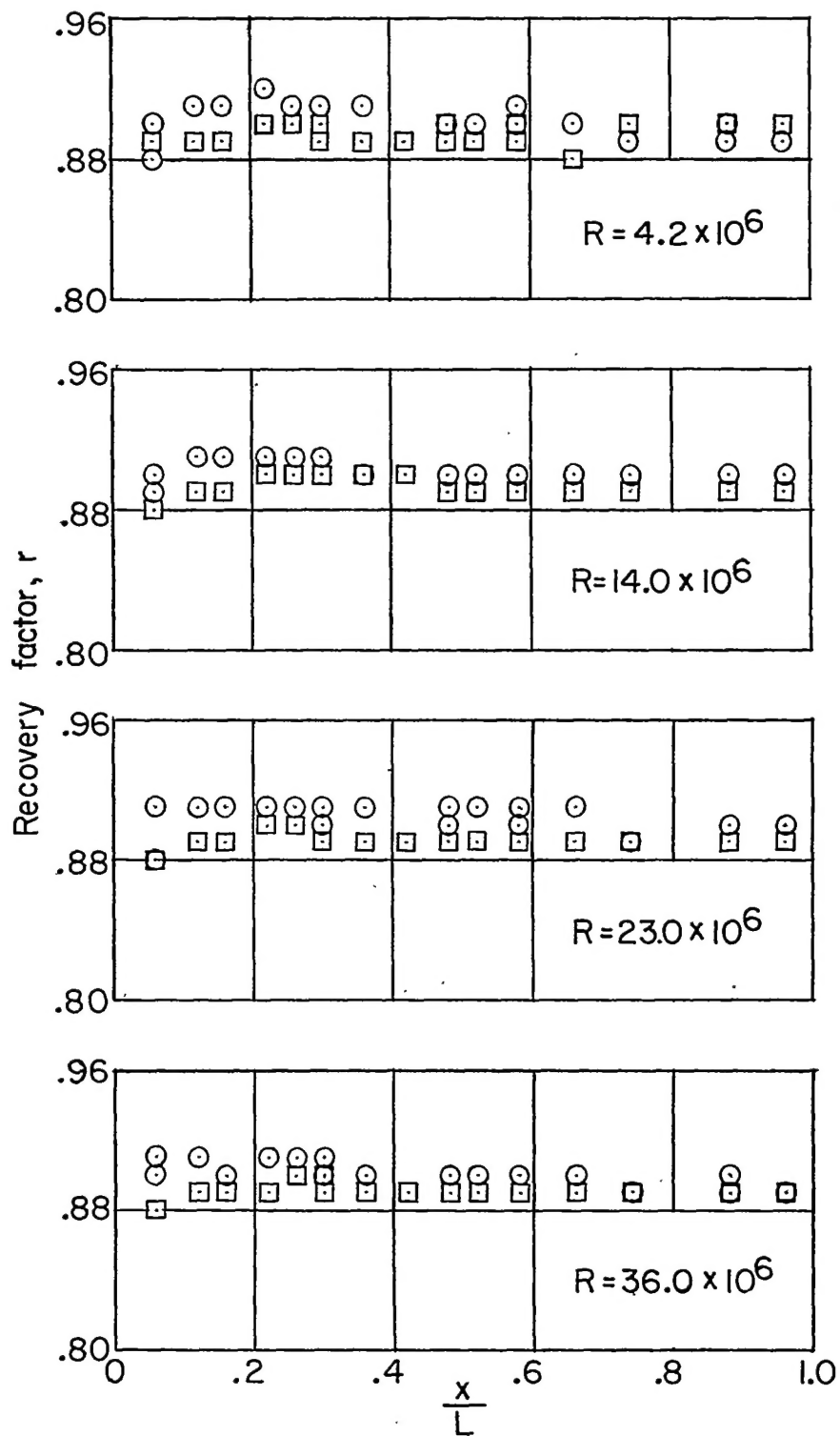
Figure 11.- Calculated variation of δ_L along the model for constant Reynolds numbers.

(a) Natural transition.

Figure 12.- Variation of recovery factor with x/L for 23- and 480-microinch-roughness models, with and without transition strip.

(b) Fixed transition.

Figure 12.- Concluded.